Modeling of HTS Dipole Magnet windings, and the influence of cable defects on Thermal and Electrical Sharing in the Cross Section

Minzheng Jiang[1], Milan Majoros[1], Edward W. Collings[1], and Mike D. Sumption[1]

[1] Department of Material Science and Engineering, Ohio State University, Columbus, USA

E-mail: jiang.1535@osu.edu

Abstract

This research explored thermal and electrical sharing, as well as quench, in the cable/composite winding cross-section of an epoxy-impregnated HEP dipole accelerator magnet using HTS （ReBCO） Cables. While HTS insert designs can vary, and in some cases, either no insulation tape windings or fully cooled cable windings are being contemplated, this design is for cables with indirect cooling (epoxy-infiltration) with specified electrical and thermal inter-cable resistances. The cables also have a defined level of defects within them, both in terms of severity and density. A direct simulation of the magnet winding with full detail in the cable structures would be far too computationally expensive to give sensible run times. However, our approach was to use results from previous modeling runs on cables to develop simple cable structures which replicated the main results of the cable properties (temperature and voltage distribution at a given current) but were averaged over length scales smaller than the cable length scale, but larger than that of the tape. These proxies were then used to construct a magnet winding cross-section, where inter-cable electrical and thermal interlayer values could be specified. Due to the complexity of structure, we simplified the epoxy layers in the model. For the present study, the magnet was designed with sixteen cables in each of the four quadrants, and one quadrant was studied. The cables themselves were constructed from thirty tapes each. The tendency for quench as a function of current was explored and compared to the performance of the isolated cables.

1. Introduction

High-energy physics (HEP) magnets play a critical role in various advanced applications, including particle accelerators, nuclear fusion reactors, and medical photon therapy [1-4]. Among the superconducting materials utilized in such magnets, rare-earth barium copper oxide (ReBCO) coated conductors [5, 6] have garnered significant attention due to their outstanding

superconducting properties, notably higher critical current densities and superior performance in strong magnetic fields [7-9].

In practical implementations, cables typically contain manufacturing defects of varying severity and distribution, influencing electrical and thermal behaviors. This research addresses the critical need to evaluate the effects of such defects on the thermal and electrical characteristics of epoxy-impregnated dipole accelerator magnets employing ReBCO cable windings. We utilized finite element method (FEM) simulations via COMSOL Multiphysics to systematically investigate the relationship between defect presence, current sharing, and quench initiation with previous research [10-12], but restricted our focus to the cables themselves. We note that the thermal boundary conditions were quite important [13]. Here we model the performance of magnets which contain the cables, and in so doing the thermal boundary conditions are naturally modified, i.e., the helium cooling is at the magnet surface rather than the cable surface.

Due to the computational limitations of directly simulating complex cable structures, we explored a multiscale modeling approach, in this case using simplified projected models which were developed based on previously synthesized cable simulation results [10, 14]. These projected models can effectively characterize key electrical and thermal properties at a medium scale, thus facilitating controlled and accurate simulation of magnet winding cross-sections. This study specifically evaluates one quadrant of a dipole magnet consisting of sixteen cables, each integrating ten stacks of three-layer cable [15, 16]. There were two defects uniformly placed in the middle layer of the three-layer cable. Each defect was 0.1mm long, spanned the entire tape width, and had an ampacity of 0.1 I_c [17]. Each cable was 4 mm μ wide, 2.25 m thick, and 3 cm long. The thickness of the epoxy was 0.75 mm between each cable and outside the magnet.

Our findings emphasize the significant impact of cable defects and thermal conditions on current sharing capabilities and magnet stability, providing essential insights for optimizing magnet designs and enhancing operational reliability.

2. Methods

We used the COMSOL Multiphysics software 3D FEM to model the cable. We used the Multiphysics model with electrostatic and temperature components in a series of steady-state simulations. The magnet is composed by 4 x 4 uniform cables which combine copper layer, YBCO layer and Hastelloy layer into one cable and we assumed the magnet was epoxy impregnated with CTD-101K with a 0.75 mm thickness between cable layers. Of course, some HTS magnet designs do not plan to use epoxy-infiltration, but we investigate here a class where this is assumed to be present. Each magnet cable contains 10 stacks of three-layer YBCO cables, each of which has two defects uniformly placed in the middle tape as shown in Figure 4. Each tape has 4mm width with 0.75μm thickness and 3cm length. The three-layer cable model and performance were studied in our previous research [10]. The details of the magnet are provided in Table I.

Table I: Magnet details

Width of cable	4 mm
Thickness of cable	2.25mm
Length of cable	3 cm
Thickness of epoxy	0.75 mm
Thickness of Cu	20 μm
Thickness of Hastelloy	30 μm
Thickness of REBCO	5 μm
Length of defect	0.1 mm
RRR value of Cu	100
n-value	15
I_c (4.2K, 8T)	596 A
J_c(4.2K, 8T)	2.98×10^{10} A/m^2
ICR	5.40×10^3 μΩ*cm^2
ITR	5.40×10^3 K*m^2/W

Figure 1 shows the 3D view and Figure 2 shows the front view of the dipole magnet model structure. Voltages were applied to the ends of the cables as circled in Figure 1, corresponding to the positive terminal, and the other end of cables are grounded. The current flows from the positive terminal to the ground terminal. The initial voltage is 0 V, and the initial temperature is 4.2 K. Heat transfer in the longitudinal direction was governed by the thermal conductivities of REBCO, Hastelloy, and copper (shown in Figure 3). The terminal (cable end) surfaces were defined as electrically conductive but thermally insulating following [18]. Heat transfer in the longitudinal direction was governed by the thermal conductivities of REBCO, Hastelloy, and copper following [19, 20].

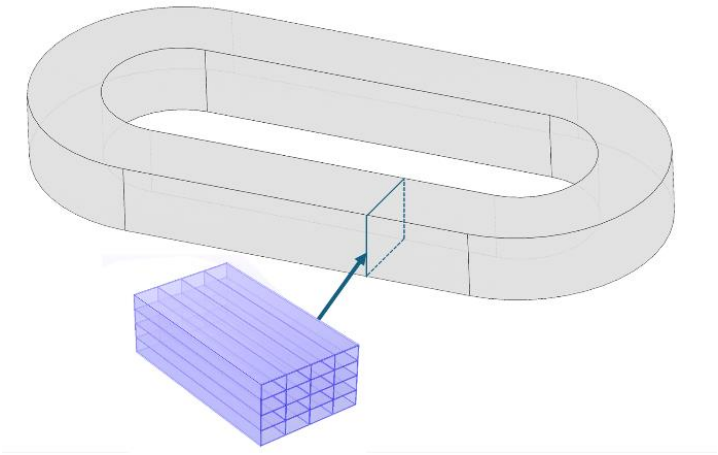

Figure 1. 3D view of the racetrack dipole magnet. The simulation model took a part of the whole racetrack dipole magnet.

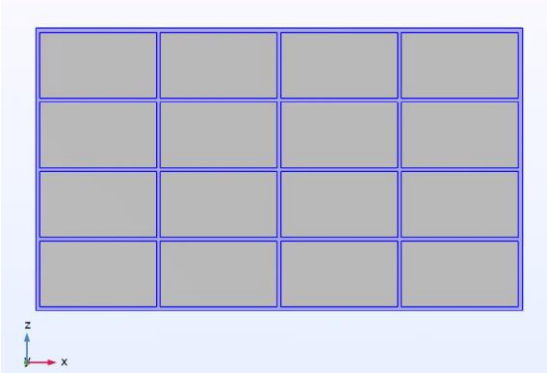

Figure 2. Cross section view of the magnet model. The grey blocks are the cables, and the blue area is the epoxy.

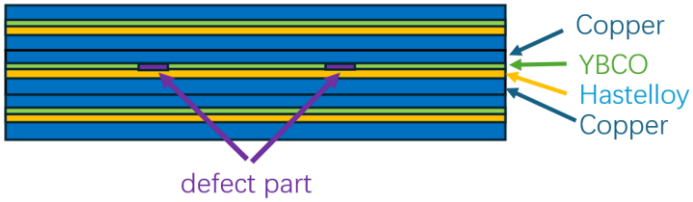

Figure 3. The structure of the cable.

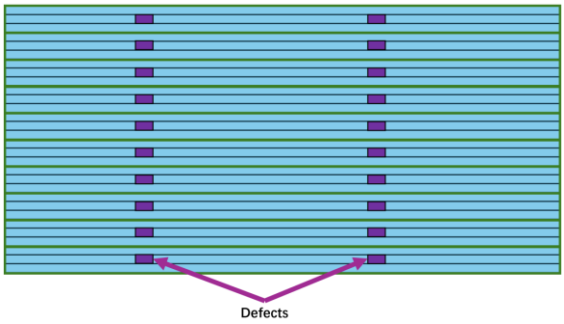

Figure 4. The side view of the magnet structure. The purple blocks are defects. The green boxes are the three-layer tape structures.

The simulation simplified the model due to the complexity. The inside epoxy was treated as thermal contact layers, and the outside epoxy was treated as thin layers with 0.75 mm thickness. The model had a symmetric plane through x-axis as shown as blue area. The final model is shown in Figure 5.

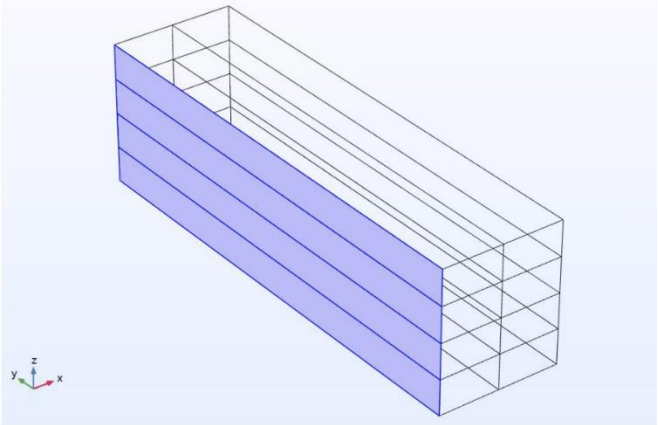

Figure 5. The simplified magnet model. Used the thermal contact and thin layer with thickness instead of real epoxy layer to decrease the complexity of the model.

The previous study from our group gave the inter-tape contact resistance (ICR) set at 5.40 × 10^3 μΩ∗cm², and the inter-tape thermal resistance was 5.54 K∗m²/W [21]. The FEM model included an extra fine mesh where the final geometry consisted of 155624 domain elements, 15428 boundary elements, and 986 edge elements. The number of degrees of freedom (DOF) solved was 457431 (plus 48624 internal DOFs). Solvers have been set up automatically by the COMSOL Multiphysics software. Physics controlled mess was set as "extremely fine". Solver tolerance setting as 1e-6 during the simulations.

The electrical conductivity of the cable is calculated as following, where the R stands for the resistance of the tape, t is the thickness, w is the width, l is the length, ρ is the electric conductivity, k is the thermal conductivity.

$$R = 2\frac{t_{cu}\rho_{cu}}{l_{cu}w_{cu}} + \frac{t_{hast}\rho_{hast}}{l_{hast}w_{hast}} + \frac{t_{YBCO}\rho_{YCBO}}{l_{YBCO}w_{YBCO}} + \eta_{CuO}l_{CuO}w_{CuO} \quad (1)$$

$$\rho = \frac{Rw_{tape}l_{tape}}{t_{tape}} \quad (2)$$

The thermal conductivity of the cable is calculated as

$$k_x = k_z = \frac{k_{cu}\times w_{cu}}{w_{cu}+w_{hast}} + \frac{k_{hast}\times w_{hast}}{w_{cu}+w_{hast}} \quad (3)$$

$$k_y = \frac{k_{cu}\times t_{cu}}{t_{cu}+t_{hast}+t_{YBCO}} + \frac{k_{hast}\times t_{hast}}{t_{cu}+t_{hast}+t_{YBCO}} + \frac{k_{YBCO}\times t_{YBCO}}{t_{cu}+t_{hast}+t_{YBCO}} \quad (4)$$

In the simulation, we applied the liquid helium pool cooling curve shown in Figure 6. The nucleate boiling peak temperature is 4.535 K, after that, cooling will transfer from nucleate boiling to film boiling accompanied by a huge decrease in the cooling power [18, 22]. Current sharing is defined as the achievable ratio of $I_{cable}/I_{cable\_nominal}$ that occurs just before thermal runaway.

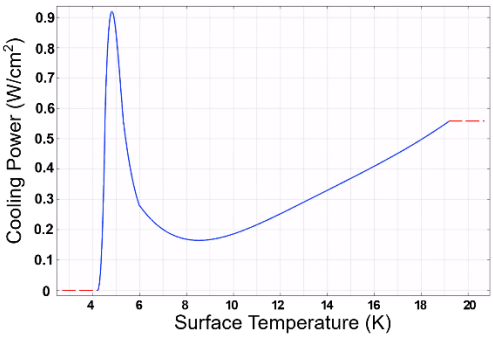

Figure 6. The liquid helium pool cooling curve. [18][22]

3. Results and Discussion

The simulation results show that the temperature inside the magnet is not the same everywhere. The middle of the magnet is hotter than the outside. This is because heat flow to the helium cooled magnet surface is restricted by the epoxy layer within the winding, as would be expected. The temperature distribution within the magnet is shown as Figure 7.

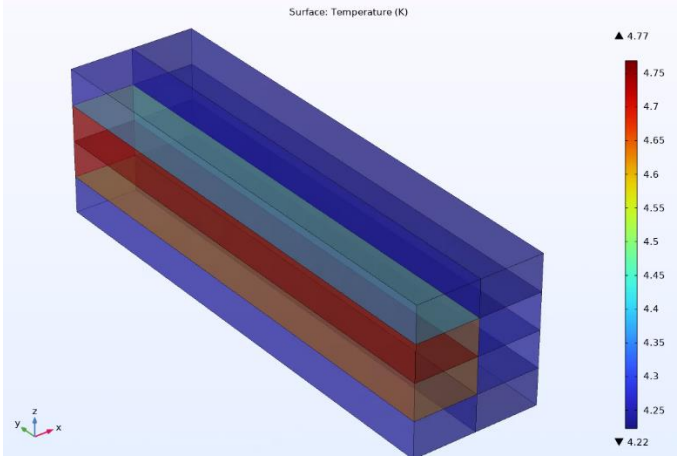

Figure 7. The temperature graph of the magnet. The center layers have higher temperature than the outside layers. The other half of the model is hidden due to the symmetric plane through x-axis. The I/Ic= 0.729, ICR=5.40 × 10^3 μΩ∗cm^2, ITR= 5.54 K∗m^2/W.

Results of the dipole model applied to the whole magnet are shown in Figure 8. The cables were connected parallel, but due to the low ITR number, there should be no big differences between the parallel connection and serial connection for the power terminal. Figure 9 shows the cross-section of the magnet. It provides a full-size view of the temperature graph of the magnet. The result corresponds to the partial magnet simulation.

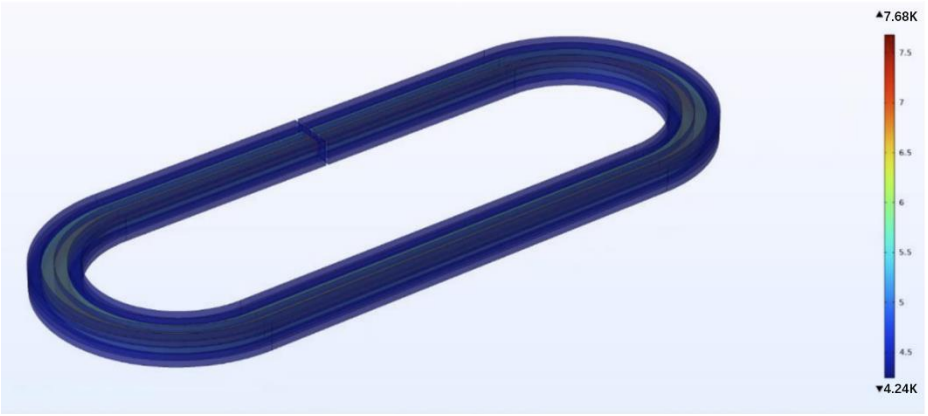

Figure 8. The full-size simulation model of dipole magnet. The magnet, composed of 4x4 epoxy-infiltrated cables, is placed in the liquid helium cooling pool. I/Ic= 0.82, ICR=5.40×10^3 μΩ*cm², ITR=5.4 K*m²/W.

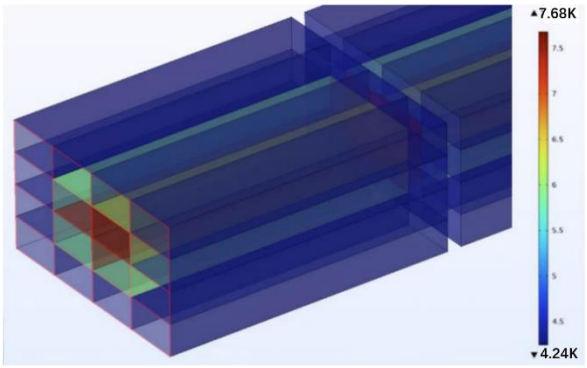

Figure 9. The cross-section view of the full-size magnet model. The center cables had higher temperatures than the outside cables.

The maximum current the magnet can carry before overheating (quenching) is about 71% of the normal current as shown in Figure 10. In contrast, a single layer of three-layer tape without epoxy can carry up to 90% of the normal current. [10] This shows that the epoxy makes it more difficult for the magnet to stay cool, causing it to overheat faster. The partial magnet simulation results match the full-size magnet well.

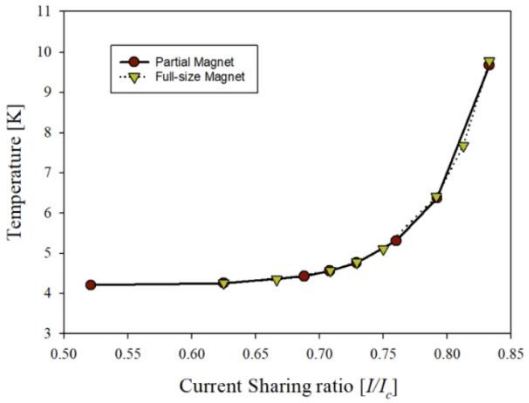

Figure 10. The temperature vs current ratio graph of partial magnet and full-size magnet.

4. Summary and Conclusion

This study analyzes the effects of cable defects and epoxy-infiltration on the thermoelectric current sharing characteristics of a high-temperature superconducting dipole magnet winding cross section. Using a simplified but effective finite element proxy model, the results show that epoxy insulation significantly reduces the maximum achievable current before the onset of quench. The maximum current sharing ratio of epoxy-impregnated cables is significantly lower than that of non-epoxy configurations. Poor ICR, ITR and high defect density would cause lower current sharing ratio. The cooling without using an insulating material was achieved with a two phases helium thermosiphon [23].

These findings highlight the importance of thermal management in optimized magnet design and emphasize that although epoxy-infiltration provides mechanical stability, it significantly inhibits heat dissipation, thus affecting the stability and reliability of the magnet. Future research should explore alternative insulation materials or cooling strategies to enhance thermal conduction and thus improve magnet performance. We have the plan to do experimental validation in future.

Acknowledgements

This work was supported by the United States Department of Energy, Office of Science, Division of High Energy Physics under Grant DE SC0011721.

References

[1] Myers C S, Sumption M D and Collings E W 2019 Magnetization and creep in YBCO tape and CORC cables for particle accelerators: value and modification via pre-injection cycle *IEEE Trans. Appl. Supercond.* **29** 1–5

[2] Bruzzone P, Fietz W H, Minervini J V, Novikov M, Yanagi N, Zhai Y *et al.* 2018 High temperature superconductors for fusion magnets *Nucl. Fusion* **58** 103001

[3] Fuger R, Eisterer M and Weber H W 2009 YBCO coated conductors for fusion magnets *IEEE Trans. Appl. Supercond.* **19** 1532–1535

[4] Brouwer L, Caspi S, Edwards K, Godeke A, Hafalia R, Hodgkinson A *et al.* 2020 Design and test of a curved superconducting dipole magnet for proton therapy *Nucl. Instrum. Methods Phys. Res. A* **957** 163414

[5] Kim W S, Park C, Park S H, Lee J, Song J B, Lee H *et al.* 2009 Magnetic field stability of a small YBCO magnet in persistent current mode *IEEE Trans. Appl. Supercond.* **19** 2194–2197

[6] Parkinson B J, Slade R, Mallett M J and Chamritski V 2013 Development of a cryogen-free 1.5 T YBCO HTS magnet for MRI *IEEE Trans. Appl. Supercond.* **23** 4400405

[7] Yanagisawa Y, Kominato Y, Nakagome H, Hu R, Takematsu T, Takao T *et al.* 2011 Magnitude of the screening field for YBCO coils *IEEE Trans. Appl. Supercond.* **21** 1640–1643

[8] Yanagisawa Y, Nakagome H, Uglietti D, Kiyoshi T, Hu R *et al.* 2010 Effect of YBCO-coil shape on the screening current-induced magnetic field intensity *IEEE Trans. Appl. Supercond.* **20** 744–747

[9] Wang X, Gourlay S A and Prestemon S O 2019 Dipole magnets above 20 T: research needs for a path via high-temperature superconducting ReBCO conductors *Instruments* **3** 62

[10] Jiang M, Xue S, Majoros M, Collings E W and Sumption M D 2025 FEM modeling of current sharing in tape stack

cables: influence of ICR, ITR, defect number, and thermal boundary conditions *IEEE Trans. Appl. Supercond.* **35** 1–5

[11] Kovacs C J, Majoros M, Sumption M D and Collings E W 2018 Quench and stability of Roebel cables at 77 K and self-field: minimum quench power, cold-end cooling, and cable cooling efficiency *Cryogenics* **95** 57–63

[12] Majoros M, Sumption M D, Xue S and Collings E W 2024 Current sharing in superconducting ReBCO cables—FEM modeling *IEEE Trans. Appl. Supercond.* **34** 1–5

[13] Peterson T J 1997 The nature of the helium flow in Fermilab's Tevatron dipole magnets *Cryogenics* **37** 727–732

[14] Xue S, Majoros M, Sumption M D, Garg T and Collings E W 2023 FEM analysis of current sharing in ReBCO coated-conductor cables for particle-accelerator applications *IEEE Trans. Appl. Supercond.* **33** 1–7

[15] Takahashi K, Amemiya N, Nakamura T, Ogitsu T, Kurusu T, Yoshiyuki T *et al.* 2011 Magnetic field design of a dipole magnet wound with coated conductor considering its current-transport characteristics *IEEE Trans. Appl. Supercond.* **21** 1833–1837

[16] Himbele J J, Badel A and Tixador P 2016 HTS dipole magnet for a particle accelerator using a twisted stacked cable *IEEE Trans. Appl. Supercond.* **26** 1–5

[17] Xu A, Jaroszynski J J, Kametani F, Chen Z, Larbalestier D C, Viouchkov Y L *et al.* 2009 Angular dependence of $J_c$for YBCO coated conductors at low temperature and very high magnetic fields *Supercond. Sci. Technol.* **23** 014003

[18] Berger A D 2011 *Stability of superconducting cables with twisted stacked YBCO coated conductors* (MSc Thesis, Massachusetts Institute of Technology)
Available at: https://dspace.mit.edu/handle/1721.1/93343 (accessed 10 May 2025)

[19] Majoros M, Sumption M D, Collings E W and Long N J 2015 Inter-strand current sharing and AC-loss measurements in superconducting YBCO Roebel cables *Supercond. Sci. Technol.* **28** 055010

[20] Ekin J W 2006 Critical-current measurements *Experimental Techniques for Low-Temperature Measurements* (Oxford: Oxford University Press) pp 353–394

[21] Xue S, Sumption M D and Collings E W 2021 YBCO coated-conductor interlayer electrical contact resistance measured from 77 K to 4 K under applied pressures up to 9.4 MPa *IEEE Trans. Appl. Supercond.* **31** 1–5

[22] Brentari E G 1965 Boiling heat transfer for oxygen, nitrogen, hydrogen and helium US National Bureau of Standards **13**

[23] Gastineau B, Donati A, Ducret J-E, Eppelle D, Fazilleau P, Graffin P *et al.* 2008 Design status of the R3B-GLAD magnet: large-acceptance superconducting dipole with active shielding, graded coils, large forces and indirect cooling by thermosiphon *IEEE Trans. Appl. Supercond.* **18** 407–410